JACS
JOURNAL OF THE AMERICAN CHEMICAL SOCIETY
pubs.acs.org/JACS
Article

Programing Chemical Communication: Allostery vs Multivalent Mechanism

Dominic Lauzon and Alexis Vallée-Bélisle*

Cite This: https://doi.org/10.1021/jacs.3c04045
Read Online

ABSTRACT: The emergence of life has relied on chemical communication and the ability to integrate multiple chemical inputs into a specific output. Two mechanisms are typically employed by nature to do so: allostery and multivalent activation. Although a better understanding of allostery has recently provided a variety of strategies to optimize the binding affinity, sensitivity, and specificity of molecular switches, mechanisms relying on multivalent activation remain poorly understood. As a proof of concept to compare the thermodynamic basis and design principles of both mechanisms, we have engineered a highly programmable DNA-based switch that can be triggered by either a multivalent or an allosteric DNA activator. By precisely designing the binding interface of the multivalent activator, we show that the affinity, dynamic range, and activated half-life of the molecular switch can be programed with even more versatility than when using an allosteric activator. The simplicity by which the activation properties of molecular switches can be rationally tuned using multivalent assembly suggests that it may find many applications in biosensing, drug delivery, synthetic biology, and molecular computation fields, where precise control over the transduction of binding events into a specific output is key.

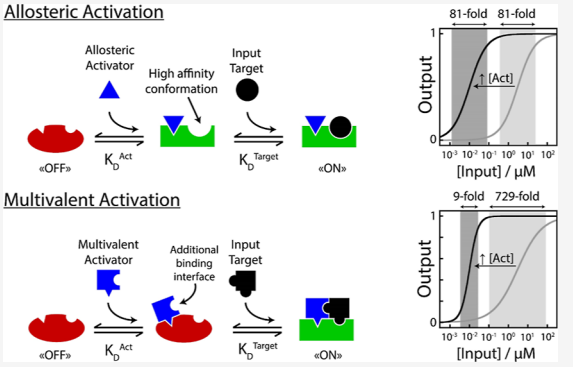

INTRODUCTION

Through billions of years of evolution, cells have developed a myriad of finely regulated nanomachines that monitor variations in their surroundings. To respond to these molecular changes, cells rely on molecular switches that exploit different mechanisms to detect and integrate these specific chemical or physical inputs (e.g., temperature, pressure, pH, small molecules, and proteins) into relevant biological activity (Figure 1, top).[1] Allosteric activation, for example, is a mechanism by which biomolecular switches become more sensitive to the presence of a molecular input (target) in the presence of an activator molecule that favors a higher affinity conformation of the switch (Figure 1, middle).[2] A better thermodynamic understanding of this biochemical mechanism has recently provided a variety of strategies to optimize the binding affinity,[3] sensitivity,[4,5] and specificity[6] of artificial nanosystems employed in biosensing[7−11] and drug delivery.[11−15]

Multivalent activation is another mechanism by which biomolecular switches become more sensitive to the presence of a molecular input (target). In this mechanism, an activator molecule binds to the molecular switch and introduces an additional binding interface (Figure 1, bottom).[16−19] Although multivalency has been exploited extensively in nature (e.g., the ribosome, antibodies, or cell surface receptors),[20−22] little is known about how this mechanism enables programing the affinity or dynamic range of molecular switches. To enable a stringent test of our understanding of this mechanism and compare its advantages and limitations with those of the allosteric mechanism, here, we have designed, modeled, and tested a simple DNA-based switch that can be activated using both mechanisms. We further demonstrate the programmable feature of the multivalent mechanisms by exploiting it to develop a programmable biosensor for antibody detection. We also discuss how this mechanism can be used to improve other artificial nanosystems.

We highlighted the potential of multivalent activation mechanisms to regulate molecular switches by exploiting the high programmability and versatility of DNA−DNA interactions. DNA offers the advantage of being easy to synthesize and modify with chemical moieties (e.g., fluorophores, quenchers, redox elements, and photoactive elements)[24,25] while having highly predictable interactions, enabling the construction of precise, well-defined nanostructures.[26] For these reasons, DNA-based systems have been used to establish the design rules behind structure switching receptors[23] and to program molecular switches through allostery[3] and ultrasensitivity.[27,28]

Received: April 19, 2023

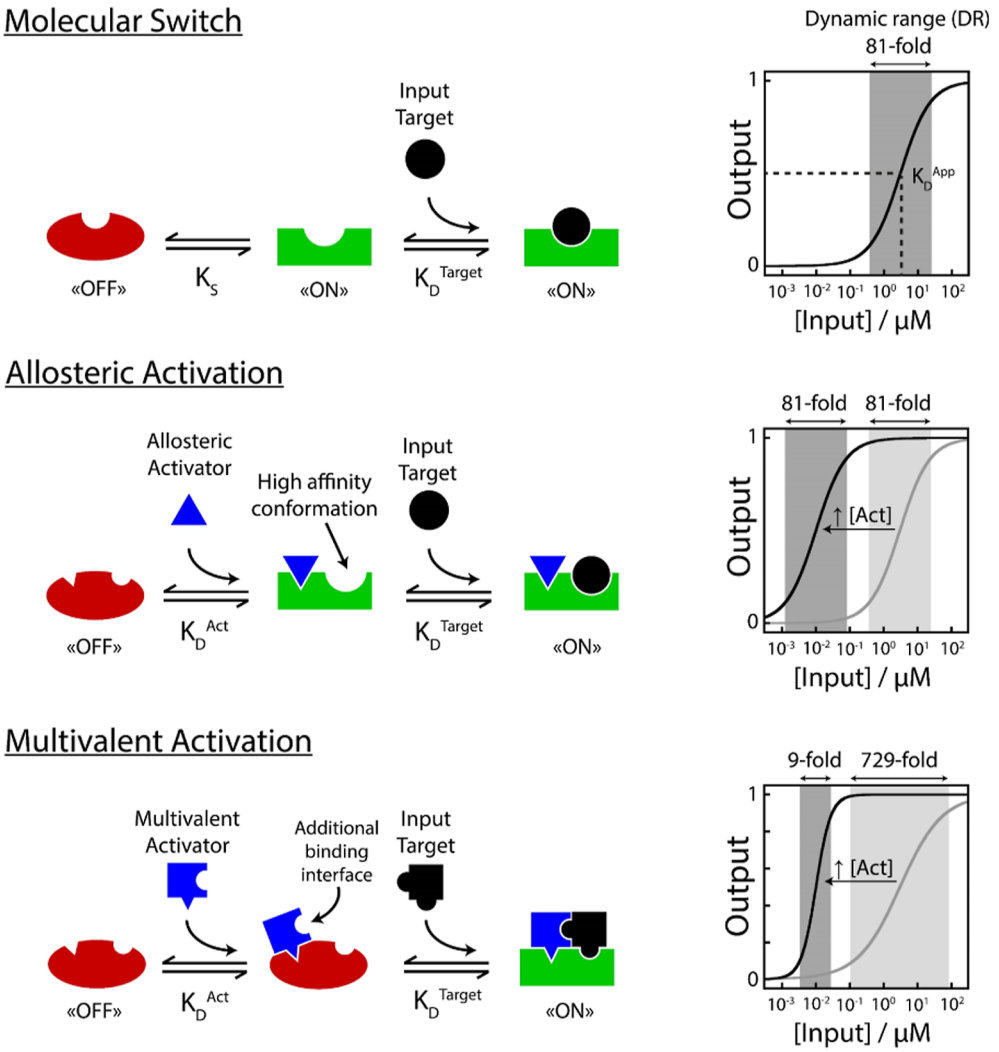

Figure 1. Engineering molecular switches with allosteric and multivalent activation mechanisms. Top. Target-binding activation of a molecular switch through a structure-switching mechanism.[23] The target binds to the high-affinity "ON-state", shifting the switch equilibrium proportionally from the "OFF-state" to the "ON-state". Middle. A molecular switch regulated via a classic allosteric activation mechanism,[2] where an allosteric activator binds and favors a higher affinity conformation of the switch, thus improving its affinity for the target (see arrow).[3] Bottom. A molecular switch regulated via a multivalent activation mechanism where a multivalent activator binds and introduces an additional interacting interface near the molecular switch, thus improving its affinity for the target (see arrow). In addition to providing a means by which the apparent K_D for the target can be programed toward lower concentration, simulations also demonstrate that this mechanism should in principle enable the programing of the switch dynamic range (see Figure S1).

RESULTS

DNA-Based Model. To understand the thermodynamic and kinetic basis of the multivalent activation mechanism, we re-engineered a DNA-based switch designed by Plaxco et al. that has been previously employed to recreate the allosteric activation mechanism (Figure S2).[3] This model switch can be easily adapted to support both mechanisms, which enables an efficient comparison between the programmability of both activation strategies. The DNA-based switch consists of a fluorescently labeled stem−loop[29] that contains a fluorophore and a quencher located next to each other when the switch conformation is in the "OFF-state" in the absence of a target. The addition of a DNA target strand complementary to the loop of this switch disrupts the stem and separates the fluorophore and quencher, thus increasing the fluorescence signal, which can then be quantified.

In the case of the allosteric activation mechanism, the activators were designed to break Watson−Crick base pairs in the stem by interacting with the "tail" added near the stem (Figure 2, top). This "strand invasion" by the activator contributes to destabilizing the "OFF-state" of the stem−loop and increasing the switching equilibrium K_S (Figure S3), thus favoring the high-affinity state by reducing the energetic penalty involved with the binding of the target to the molecular switch.[23] To recreate a multivalent activator mechanism, we also designed multivalent activators to interact with the "tail" of the switch. However, instead of favoring the "ON-state" of the switch, the multivalent activator simply provides an additional interacting interface for the target (Figure 2, bottom). This new interacting interface increases the affinity of the target for the switch through the formation of a three-way junction assembly.[30]

Allosteric versus Multivalent Activation Mechanisms. We first validated the impact of these two distinct activators on the equilibrium of the switch (Figures 2 and S3). To do so, we characterized the switching equilibrium of our DNA-based

https://doi.org/10.1021/jacs.3c04045
J. Am. Chem. Soc. XXXX, XXX, XXX−XXX

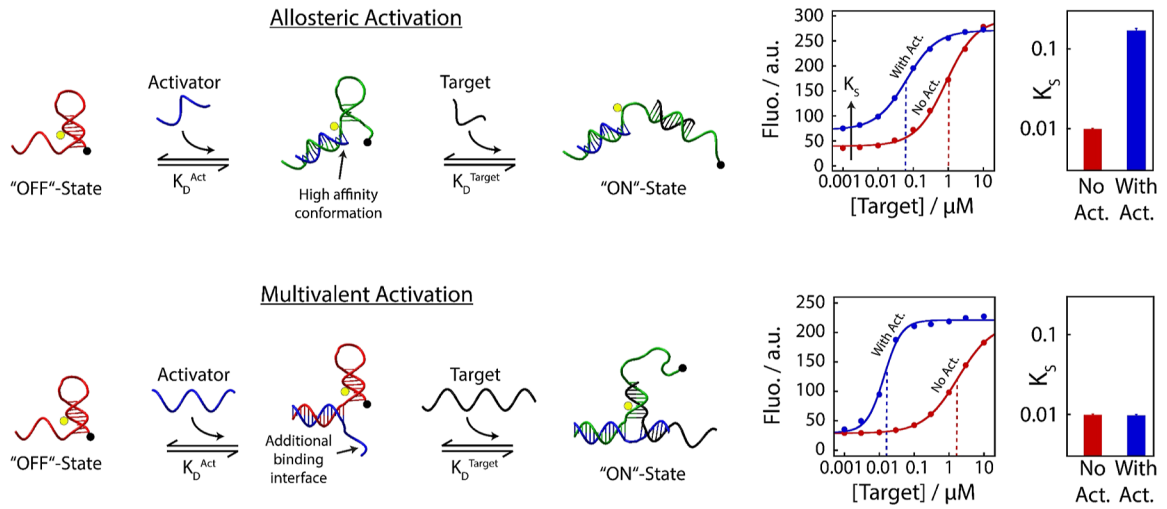

Figure 2. DNA molecular switch modulated via an allosteric or a multivalent mechanism. Top. A DNA switch controlled via an allosteric activator (blue strand).[3] In this model proposed by Plaxco et al., the DNA activator invades and destabilizes the stem of a fluorescent DNA switch, thus favoring the equilibrium (K_S) toward the "ON-state" (see arrow) and improving target affinity. The increased "ON-state" population is confirmed by an increase in the fluorescence background of the switch (blue curve). Bottom. A DNA switch controlled by a multivalent activator (blue strand). Upon binding to the switch, this DNA activator introduces an additional hybridization interface that increases the affinity of the target (see arrow). In contrast to the allosteric activator, the multivalent activator does not alter the switching equilibrium (similar background fluorescence in the absence and presence of the activator). The yellow circle represents an FAM moiety chemically attached to a thymine base, while the black circle represents a BHQ-1 moiety chemically attached at the 3′ extremity. Both were introduced as a labeling strategy to determine the conformational state of the switch. See Figures S4 and S5 for the calculation of K_S.

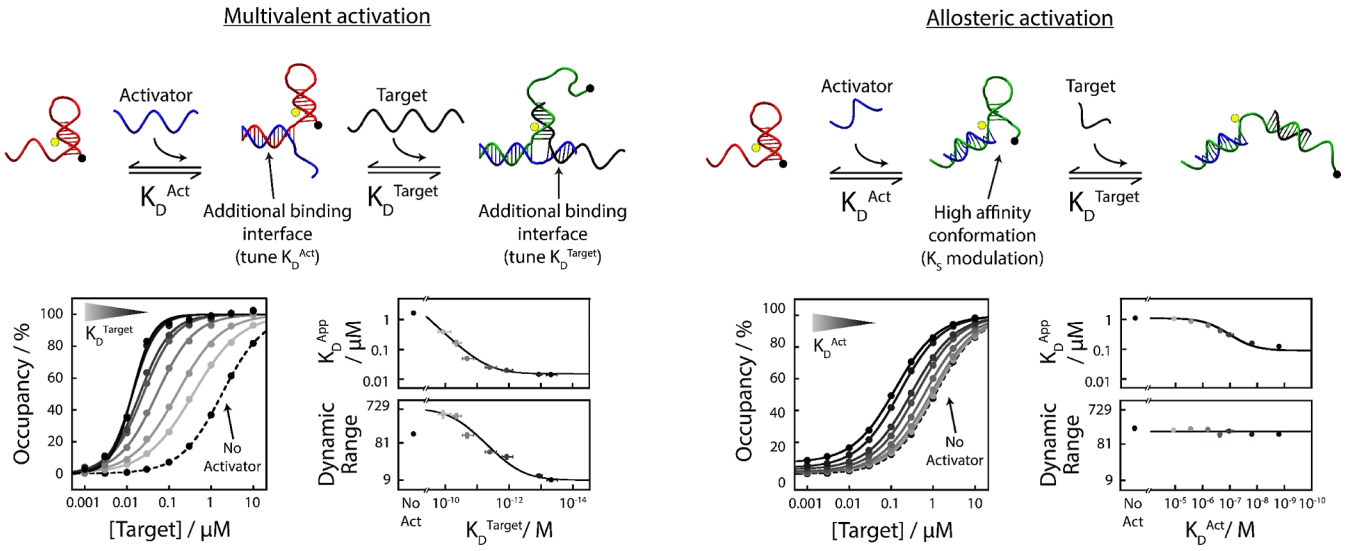

Figure 3. Programing a DNA-based switch using multivalent and allosteric activators. *Multivalent activation.* We designed multivalent activators with different lengths of binding interfaces for either the switch or the target, thus enabling the tuning of the K_D^{Act} and the K_D^{Target}, respectively. Tuning K_D^{Target} enables the programing of the K_D^{App} from 1.7 ± 0.1 μM (No Act) to 0.0142 ± 0.0003 μM (≈15 nM, i.e., ligand depletion regime[32,33]) and the dynamic range of the switch from 729 to 9. See Figure S7 for the tuning of K_D^{Act}. *Allosteric activation.* We designed allosteric activators with different lengths, thus enabling tuning the K_D^{Act} and the K_S of the switch. In contrast to the multivalent activation, allosteric activators enable programing the affinity of the switch for its target (K_D^{App}) by only 1 order of magnitude from 1.11 ± 0.03 μM (No Act) to 0.123 ± 0.004 μM while having no impact on the dynamic range of the switch (DR = 185 ± 29, in average). All binding curves were performed in triplicate (n = 3) using 30 nM switch and 30 nM activator. See Figure S10 (K_D^{Act}, multivalent), Figure S11 (K_D^{Target}, multivalent), and Figure S13 (K_D^{Act}, allostery) for raw fluorescence data. Binding curves were fitted by using the Hill equation. The K_D^{App} and dynamic ranges of the multivalent system were well-fitted by our mathematical equations (eqs 1 and 2). The K_D^{App} and dynamic ranges of the allosteric system were fitted using previously validated mathematical models.[3]

switch using urea denaturation procedures (Figure S4).[31] We measured a ΔG of 3.00 ± 0.06 kcal·mol^{-1}, which led to a switching constant (K_S) of 0.0089 ± 0.0008, meaning that 99% of the switch remained in the "OFF-state" in the absence of activators or targets. As expected, upon binding to the switch, the allosteric activator alters the switching equilibrium of the switch from K_S = 0.0089 ± 0.0008 to 0.17 ± 0.01, as confirmed by the increase in the initial fluorescence of the switch.[3,23] Favoring the equilibrium toward the "ON-state" (only 85% of the switch remains in the "OFF-state") also improved the apparent affinity of the switch by 16-fold (from 1.14 ± 0.03 to 0.068 ± 0.004 μM).

https://doi.org/10.1021/jacs.3c04045
J. Am. Chem. Soc. XXXX, XXX, XXX−XXX

In contrast, we confirmed that the multivalent activator did not alter the switching equilibrium. Indeed, the latter remained unchanged (K_S = 0.0092 ± 0.0009) since no impact on the initial background signal of the switch was observed. We also found that the additional interacting interface provided by the activator also improved the apparent affinity of the switch by up to 100-fold (from 1.7 ± 0.1 to 0.0142 ± 0.0003 μM). We further looked at the impact of longer allosteric and multivalent activators and confirmed that no matter the length of the additional interacting interface, multivalent activators never affected the switching equilibrium (Figure S5). Interestingly, we also noted that multivalent activators drastically affected the dynamic range of the molecular switch. Indeed, while the dynamic range of an allosterically activated switch remains unchanged, a multivalently activated switch displays a narrower dynamic range (from DR = 153 ± 10 to DR = 10 ± 1). Finally, we also observed that in the absence of activators, the switch displays a similar affinity for both targets employed in the different strategies (red binding curves, K_D = 1.11 ± 0.03 and 1.7 ± 0.1 μM, respectively, in the absence of activators). These experiments also suggest that in contrast to the allosteric activation strategy that typically proceeds via a population shift model,[3,4] the multivalent activation strategy does not involve changes in the state of the switch (i.e., the switch remains in its "OFF-state" even in the presence of the activator). Instead, the activator provides an additional interface that enables the target to directly bind the "OFF-state" of the switch, a strategy reminiscent of the induced fit mechanism where the ligand binds the "OFF-state" first. This multivalent activation strategy is also evocative of the associative toehold-mediated strand displacement strategy where an associative domain brings a toehold domain in close vicinity of a branch migration domain.[34,35]

Mathematical Validation of the Multivalent Mechanism. Having determined that the multivalent activator behaved as expected (Figures 2 and S3), we then explored quantitatively its programing abilities by determining the mathematical equations describing its function. Multivalent activation is expected to work via a two-step equilibrium. First, the binding of the multivalent activator to the switch (Figure 3, left, K_D^{Act}) increases the interacting interface for target binding, which, in turn, improves its affinity (Figure 3, left, K_D^{Target}).

We defined two parameters to describe the shape of the binding curves: 1) the K_D^{App} (the apparent dissociation constant, i.e., the concentration of targets where 50% of the switch is active) and 2) the dynamic range (DR) (i.e., the range of concentration over which the switch goes from 10% active to 90% active). These two parameters can be defined in relation to K_D^{Act} and K_D^{Target} following the two equations below

$$K_D^{App} = \frac{[Act]_T}{2}\left(1 + \frac{K_D^{Target}}{[Act\text{-}Sw]_{50\%}}\right) \quad (1)$$

$$DR = 9\frac{\left(1 + \frac{K_D^{Target}}{[Act\text{-}Sw]_{90\%}}\right)}{\left(1 + \frac{K_D^{Target}}{[Act\text{-}Sw]_{10\%}}\right)} \quad (2)$$

where $[Act\text{-}Sw]_{x\,\%}$ is the concentration of the activated switches when x % of the target is bound and it can be calculated as follows

$$[Act - Sw]_{x\,\%} = \frac{K_D^{Act} + 2[Act]_T(1-x) - \sqrt{(K_D^{Act})^2 + 4[Act]_T K_D^{Act}(1-x)}}{2} \quad (3)$$

where $[Act]_T$ is the total concentration of activators and x is either 0.1, 0.5, or 0.9 (10, 50, and 90% respectively). Of note, in this simplified scenario, the concentration of activators is equal to the concentration of switches (see the Supporting Information for the case where the concentration of activators is not equal to the concentration of switches). Overall, these two equations reveal multiple ways to program the K_D^{App} and the DR by either tuning the K_D^{Act}, tuning the K_D^{Target}, or changing the concentration of activated switches via a change in the concentration of activators and switches.

Multivalent activation: Tuning K_D^{Act}. We first designed activators of different lengths to increase the size of its interacting interface with the switch (from 8 to 14 nucleotides), which increases the affinity of the activator for the switch (K_D^{Act}, see Figure S6). To ensure that we simply looked at the effect of K_D^{Act} on the activation of the switch, we kept the interacting interface between the activator and the target constant (13 nucleotides, K_D^{Target} = 0.05 ± 0.02 pM). In the absence of activators, the switch displayed a K_D of 1.7 ± 0.1 μM with a dynamic range of 153 ± 10 (n_H = 0.87 ± 0.01) (Figure S7). When employing an activator with a short-binding domain for the switch (8 nt, K_D^{Act} = 793 ± 362 μM), only 30 ± 1% of trimer forms and 70% of the switch remain unaffected by the activator (i.e., biphasic binding curve). In contrast, when our strongest activator is used (14 nt, K_D^{Act} = 0.39 ± 0.01 μM), all switches form a trimer. In such a case, the binding curve displays a K_D^{App} = 14.2 ± 0.3 nM (1/2 [switch], ligand depletion regime[32,33]) and a DR of 9.2 ± 0.2. Interestingly, when using an activator of 9 nt, we can also program the detection of the target over an extended dynamic range (DR ≈ 10^3) by exploiting the presence of two switch populations: one "high affinity" activated switch and one "low affinity" unbound switch (biphasic transition, Figure S8).[36] Overall, K_D^{Act} dictated the extent or the amount of switch that will be activated (i.e., [Act-Sw]). As a rule of thumb, to ensure proper activation using the multivalent mechanism, K_D^{Act} must be kept below the affinity of the target in the absence of an activator (e.g., K_D^{Act} 14nt = 0.39 ± 0.01 μM < 1.7 ± 0.1 μM).

Multivalent activation: Tuning K_D^{Target}. We then designed activators of different lengths to increase the size of its interacting interface with the target (from 7 to 13 nucleotides), which in turn increases the affinity of the target toward the switch−activator complex (K_D^{Target}, see Figure S9). To ensure that we simply looked at the effect of K_D^{Target} on the activation of the switch, we kept the interacting interface between the activator and the switch constant (14 nucleotides, K_D^{Act} = 0.39 ± 0.01 μM). Adding a multivalent activator that contains an additional interacting interface for the target of 7 nt (K_D^{Target} = 0.12 ± 0.05 nM) produced a switch that opened at 4 times less target concentration (K_D^{App} = 0.39 ± 0.05 μM) with an extended dynamic range reaching up to 729-fold (DR = 514 ± 118) (Figure 3, left). When increasing the length of this activator by up to 6 extra nucleotides (from 7 to 13 nt, K_D^{Target} = 0.05 ± 0.02 pM), we observed a 100-fold decrease in K_D^{App} until reaching the ligand depletion regime (K_D^{App} = 15 nM = 1/2 [switch]).[32,33] Furthermore, we found that the dynamic range of the switch bound to the longest activator (13 nt) is now reduced to a narrow, "cooperative-like", 9-fold

https://doi.org/10.1021/jacs.3c04045
J. Am. Chem. Soc. XXXX, XXX, XXX−XXX

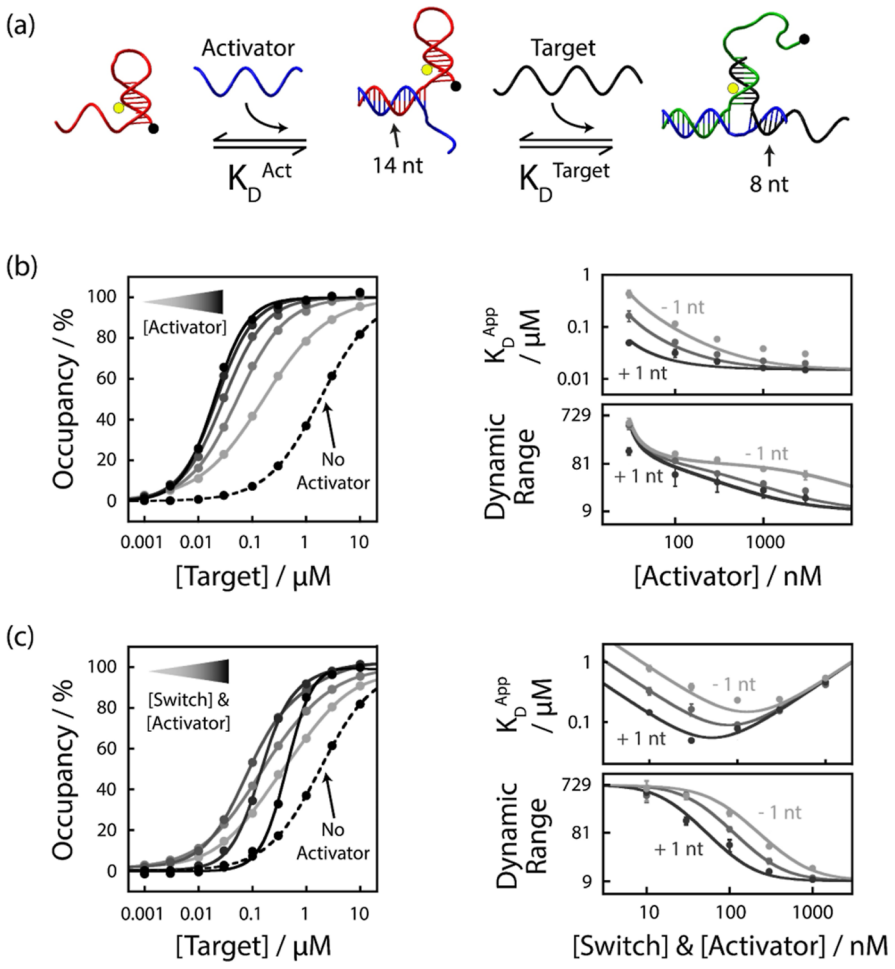

Figure 4. Programing the affinity and dynamic range of molecular switches by tuning the concentration of multivalent activators. (a) Here, we show the effect of varying the concentration of activators and switches using the activator displaying a 14-nucleotide binding interface with the switch and an 8-nucleotide binding interface with the target. In this experiment, the concentration of switches (30 nM) is much higher than the K_D^{Target} (45 ± 13 pM), leading to a ligand depletion regime and a narrow dynamic range when the switch becomes fully activated. (b) Increasing the concentration of activators above the concentration of switches (30 nM) reduces both the K_D^{App} and the dynamic range. (c) Increasing altogether the concentration of activators and switches provides a way to program K_D^{App} in a bell-shaped pattern, whereas the dynamic range is narrowed following a sigmoidal pattern. All binding curves were performed in triplicate (n = 3). See Figures S14 and S15 for raw data. Binding curves were fitted using the Hill equation. All K_D^{App} values and dynamic ranges were well-fitted as shown in eqs 1 and 2.

dynamic range, a behavior also expected from a molecular system under a ligand depletion regime.[32,33]

Multivalent versus Allosteric Activation. In contrast to the multivalent activation mechanism, the same level of programing could not be achieved by using allosteric activators (Figure 3, right). Although allosteric activators with various K_D^{Act} values (Figure S12) allowed us to modify the K_D^{App} by 10-fold (from 1.11 ± 0.03 to 0.123 ± 0.004 μM), they did not allow the tuning of the dynamic range (DR = 185 ± 29, in average). As demonstrated in previous studies,[3] the extent to which an allosteric activator can improve the binding affinity of a molecular switch is limited by the affinity of the target for the "OFF-" and "ON-state" of the switch. In contrast, the extent to which a multivalent activator can improve the binding affinity of a molecular switch does not depend on the conformation of the switch but rather is directly proportional to the additional energy provided by the new interacting interface. Since the allosteric activation mechanism was previously thoroughly validated mathematically and experimentally,[3,10,37,38] we went on to further explore the programing ability of the multivalent activation strategy.

Multivalent activation: Effect of Component Concentration. The activity of a multivalently activated switch can also be tuned by simply varying the concentrations of its components. For example, this could be done by either changing the concentration of activators or by changing together the concentration of activators and switches (Figure 4a). To validate these predictions quantitatively, we performed experiments using the activator with a 14-nucleotide binding interface with the switch (K_D^{Act} = 0.39 ± 0.01 μM) and an 8-nucleotide binding interface with the target (K_D^{Target} = 45 ± 13 pM).

We first demonstrated that we can program the K_D^{App} and the dynamic range of the switch by simply tuning the concentration of the activators (Figure 4b). At low concentrations of activators (e.g., 30 nM), the switch is not fully bound to the activator, and trimeric assembly occurs at higher target concentrations (K_D^{App} = 0.16 ± 0.04 μM) with an extended dynamic range (DR ∼ 729). At higher concentrations of activators (e.g., 3000 nM), all switches become bound to the activator and now display a K_D^{App} = 0.020 ± 0.001 μM. This K_D^{App} corresponds to half the concentration of

https://doi.org/10.1021/jacs.3c04045
J. Am. Chem. Soc. XXXX, XXX, XXX−XXX

switches ([Sw] = 0.030 μM) given that it remains under a depletion regime, thus leading to a narrow dynamic range (DR ~ 9). Shorter and longer activators, which display lower and higher K_D^{Target} values, respectively, also enable further tuning possibilities (Figure 4b, right).

We also demonstrated that we can program the K_D^{App} and the dynamic range of the switch by tuning the concentrations of both activators and switches (Figure 4c). At low concentrations of the switch−activator complex (e.g., 10 nM), the switch is not bound to the activator, and trimeric assembly occurs at high target concentrations (K_D^{App} = 0.33 ± 0.05 μM) with an extended dynamic range (DR ~ 729). As we increased the concentration of switch−activator complexes (e.g., 100 nM), the binding of the target occurred at a lower concentration (K_D^{App} = 0.090 ± 0.002 μM) with a reduced dynamic range (DR = 96 ± 9). At higher concentrations of the switch−activator complex (e.g., 1000 nM), the ligand depletion regime pushes back the K_D^{App} to higher values (e.g., 0.417 ± 0.004 μM), corresponding to nearly half of the concentration of switches being used (i.e., 500 nM). As expected from the depletion regime, such conditions provide a narrower switch opening (DR ~ 9).[32,33]

Shorter and longer activators also enable programing the activation profile of the switch (Figure 4c, −1 and +1 nt). For instance, a weaker multivalent activator (−1 nt, K_D^{Target} = 118 ± 51 pM) displaces the concentration-dependent profile of K_D^{App} and dynamic range toward higher concentrations, while a stronger multivalent activator (+1 nt, K_D^{Target} = 21 ± 8 pM) displaces them toward lower concentrations. A multivalent activator also enables independent programing of the dynamic range from its K_D^{App} (Figure S16). For example, a 100-fold increase in concentration (from 10 to 1000 nM) led to activation that occurred at a similar concentration (K_D^{App} = 0.33 ± 0.05 vs 0.417 ± 0.004 μM, respectively) but with a 40-fold variation in the dynamic range (DR = 446 ± 117 vs 10.4 ± 0.4, respectively).

In summary, all these experimental results were well-modeled by our mathematical equations (eqs 1 and 2). This illustrates how multivalent activators enable precise programing of molecular switches at different target concentrations (K_D^{App}) with the desired sensitivity (DR) by simply tuning the K_D^{Act}, the K_D^{Target}, or the concentration of its constituents.

Tuning the Kinetics. Multivalent activators also possess a remarkable ability to program the half-life of the "ON-state" of a switch when compared to their allosteric counterpart (Figures S17−S19). For example, when destabilizing the stem and favoring the high-affinity "ON-state", the allosteric activator enables slight acceleration of the binding of the target (k_{on}) from 0.30 ± 0.02 to 0.536 ± 0.007 $s^{-1}\cdot\mu M^{-1}$ while also slowing down its dissociation rate (k_{off}) from 0.078 ± 0.008 to 0.0140 ± 0.0008 s^{-1}, both by less than 1 order of magnitude. In the case of the multivalent activator, however, the additional interface does not alter the conformational state of the switch, and thus, the binding of the target remains rate-limited by its invasion into the stem (all k_{on} values are 0.027 ± 0.002 $s^{-1}\cdot\mu M^{-1}$). The additional interface, however, considerably impacts the dissociation of the activated switch complex since more base pairs need to be broken for dissociation to occur, and k_{off} thus decreases by up to 2 orders of magnitude from 0.035 ± 0.002 to (2.4 ± 0.6) × 10^{-4} s^{-1}. Therefore, while an allosterically activated switch displays association and dissociation rates linked to its switching equilibrium (K_S), a multivalently activated switch only sees its deactivation rate impacted, which provides a way to precisely program the half-life and residence time of the activated state of the switch without changing its rate of activation.

Multivalently Activated Biosensors. In order to test the universality of the multivalent strategy to other biomolecules, we adapted our DNA switch for the detection of antibodies (Figure 5).[39−42] To do so, we replaced the DNA target binding

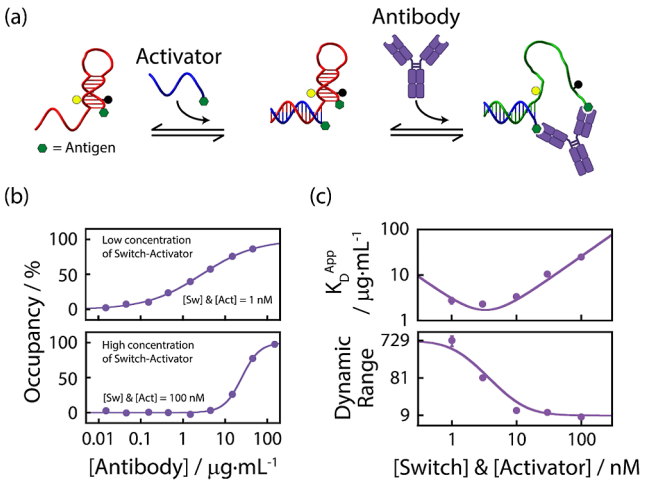

Figure 5. Programing the dynamic range of an antibody sensor using a multivalent activator. (a) In order to test the universality of the multivalent activation strategy, we replaced the DNA binding interface with biotins, a well-characterized antigen. When bound to the switch, the activator provides a second binding site for an antibiotin antibody, leading to an improved affinity for the switch. (b) As expected, at low concentrations of activators and switches (i.e., 1 nM), antibody detection proceeds over an extended dynamic range (K_D^{App} = 2.8 ± 0.5 $\mu g\cdot mL^{-1}$ and DR = 728 ± 211). At high concentrations of activators and switches (i.e., 100 nM), antibodies are detected at higher concentrations with a much narrower dynamic range (K_D^{App} = 25 ± 1 $\mu g\cdot mL^{-1}$ and DR = 8.3 ± 0.6). (c) All K_D^{App} and DR values obtained at different concentrations of switches and activators (from 1 to 100 nM) are well-modeled by eqs 1 and 2. See Figure S22 for raw data. Binding curves were fitted using the Hill equation, and errors were obtained from the fitting.

sites on the switch and activator with biotins, which is a well-characterized antigen (Figure 5a). When bound to the switch, the multivalent activator provides an additional antigen for the antibody near the first one. Upon binding to the antigen of the switch, binding of the antibody to the second antigen is favored through stem opening, therefore generating an increase in fluorescence (antigen binding sites of an antibody are typically separated by 12 nm).[39] Of note, we observed that the binding of the antibody to the activated switch does not fully unfold the switch but rather moves the quencher further apart from the fluorophore, providing an increase in the fluorescence signal of around 50% (Figure S20).

As observed for the DNA-activated switch, we also demonstrated the high programmability of the antibody switch (Figure 5b,c). To ensure that the trimeric assembly between the switch, the activator, and the antibody remains energetically favorable, we employed our strongest multivalent activator (14 nucleotides, K_D^{Act} = 0.39 ± 0.01 μM, Figure 3b). We then evaluated the affinity of the antibody for its antigen (K_D^{Ab} = 0.23 ± 0.04 μM; Figure S21) and found it to be close to the affinity of our DNA multivalent target (1.14 ± 0.03 μM, Figure 2). As expected, when using a low

https://doi.org/10.1021/jacs.3c04045
J. Am. Chem. Soc. XXXX, XXX, XXX−XXX

concentration of activators and switches (1 nM, Figure 5b, top), the antibodies were detected over an extended dynamic range (DR = 728 ± 211). In contrast, when a higher concentration of activators and switches was used (100 nM, Figure 5b, bottom), the antibodies were detected over a narrower dynamic range (DR = 8.3 ± 0.6), in agreement with the ligand depletion regime. The concentration-dependent profiles (K_D^{App} and DR) of this antibody detection system were also well-fitted by our mathematical model (Figure 5c). Of note, we noticed that when we employed a low concentration of activators and switches, the antibodies can sequester the activator and the switch through the formation of dimeric traps (Figure S23). This leads to a slower kinetics of activation since one has to wait for the dissociation of the switch (or activator) to form the trimeric activated switch complex.[30]

We also evaluated the effect of increasing the affinity of the antigen for its target molecule (K_D^{Target}). Although the affinity of the antigen for an antibody is hardly programmable, we can still evaluate the effect of K_D^{Target} using streptavidin, a target molecule that displays a stronger affinity for biotin ($K_D^{Strep} \approx 10^{-14}$ M). When detecting streptavidin with the same switch, we observed that all binding curves displayed low K_D^{App} and even more narrowed dynamic ranges, consistent with the ligand depletion regime and the four biotin-binding sites (Figure S24). Overall, these experiments illustrate how multivalent activators can help program the dynamic range of biosensors that target antibodies or other proteins displaying multiple binding sites. We also expect this strategy to be useful for the design of aptamer-based biosensors (e.g., aptamers or DNA strands that bind to multivalent proteins,[43−45] bivalent aptamers,[46,47] or split aptamers[48,49]).

DISCUSSION

To enable a stringent test of our understanding of two molecular languages enabling chemical communication, allostery and the multivalent mechanism, here, we have designed, modeled, and tested a simple DNA-based switch that can be activated using both mechanisms. Compared to allosteric activators that displace the switching equilibrium,[3,4,8,9] multivalent activators simply consist in adding a novel interacting interface for the target. Remarkably, this simple addition enables the programing of both the affinity and dynamic range of switches from a narrow 9-fold to an extended 729-fold dynamic range. In comparison, narrow or extended dynamic ranges in allosteric systems can only be obtained by engineering homotropic allosteric mechanisms (energetically connected binding interfaces)[4,5] or by combining multiple switches,[37,50] respectively. Multivalent activators also enable programing of the dynamic range of a switch independently from its apparent affinity, leading to precise control over the activation threshold and the sensitivity of molecular switches. Furthermore, multivalent activators provide a way to rationally tune the half-life of the "ON-state" of the switch (k_{off}) while not affecting its activation rate (k_{on}), which can still be optimized through an allosteric activation mechanism if needed. Ultimately, the ability to rationally control the properties of molecular switches through the formation of a multivalent assembly can find many applications in DNA-based nanotechnologies to improve the binding efficiency of DNA switches, to modulate the drug release properties of DNA cargo, to increase the residence time of activated switches, or to program DNA-based computation.[50,51]

More specifically, we also demonstrated how the multivalent activation strategy can be used to program and optimize other nanosystems. For example, by adding a multivalent activator mechanism to a previously reported antibody switch,[39] we demonstrated how this switch could be further programed to detect antibodies over the desired, optimal dynamic range. We believe that such a multivalent strategy could easily be adapted for the detection of any type of molecules by employing their respective recognition elements (e.g., DNA, RNA, peptides, small molecules, etc.). For instance, the detection of antibodies can be diversified by attaching peptides instead of small molecules (e.g., biotin). Bivalent aptamers could also be reprogramed to detect specific molecular targets (e.g., for thrombin detection, a switch can be fused to the TBA aptamer, while the multivalent activator can be fused to the HD22 aptamer).[46,47] Split aptamer[48] or split protein[52] systems could also benefit from multivalent activation by providing a programmable associative domain that promotes the reconstitution of the two fragments in the presence of its molecular target. Finally, the controlled release of molecular cargo[53] or bivalent drugs such as PROTAC[54] could also benefit from the longer residence time in the "ON-state" (i.e., $\tau = 1/k_{off}$) provided by multivalently activated switches.[55]

Such a multivalent mechanism may also have broad repercussions in the design of *de novo* protein-based assemblies, where such assemblies are often designed through a modular approach of linking multivalent interacting domains together.[18] In addition, we also believe that a better understanding and comparison of the allosteric and multivalent mechanisms provide new insights to better understand the evolution of biomolecular receptors and switches and why some have selected multivalency over allostery (e.g., the Notch-1 transcriptional complex, the assembly of the 30S ribosome, and β-interferon enhanceosome).[56−58]

ASSOCIATED CONTENT

Supporting Information

The Supporting Information is available free of charge at https://pubs.acs.org/doi/10.1021/jacs.3c04045.

Materials and methods; DNA sequences; figures showing the multiple interacting pathways of a multivalently activated switch, comparison between the original switch and our switch, switching equilibrium of the inactivated, allosterically activated, and multivalently activated switch, and the stability of the switch; determination of the affinity of the activators, multivalent targets for the activated switch, and the antibody for its antigen; determination of the kinetic constants; how to program the multivalently activated switches using K_D^{Act}; how to program the activation/deactivation kinetics of molecular switches; tables of the impact of the allosteric activator and multivalent activator on the switching equilibrium (K_S), multivalent K_D^{Act}, multivalent K_D^{Target}, allosteric K_D^{Act}, and kinetic parameters (k_{on} and k_{off}); raw data; and fitting equations (PDF)

AUTHOR INFORMATION

Corresponding Author

Alexis Vallée-Bélisle − *Département de Chimie, Laboratoire de Biosenseurs et Nanomachines, Université de Montréal, Montréal QC H2V 0B3, Canada;* orcid.org/0000-0002-5009-7715; Email: a.vallee-belisle@umontreal.ca

https://doi.org/10.1021/jacs.3c04045
J. Am. Chem. Soc. XXXX, XXX, XXX−XXX

Author

Dominic Lauzon − *Département de Chimie, Laboratoire de Biosenseurs et Nanomachines, Université de Montréal, Montréal QC H2V 0B3, Canada;* orcid.org/0000-0002-7513-3233

Complete contact information is available at: https://pubs.acs.org/10.1021/jacs.3c04045

Author Contributions

The manuscript was written through contributions of all authors. All authors have given approval to the final version of the manuscript.

Notes

The authors declare no competing financial interest.

■ ACKNOWLEDGMENTS

A.V.B. acknowledges the Natural Sciences and Engineering Research Council of Canada (Conseil de Recherches en Sciences Naturelles et en Génie du Canada)—RGPIN-2020-06975—for funding this work. A.V.-B. is the Canada Research Chair in Bioengineering and Bionanotechnology, Tier II. D.L. acknowledges Le Fonds de recherche du Québec−Nature et technologies for financial support during its doctoral study—grant numbers: 256330 and 290101. The authors would like to thank J. Pelletier and M. Merkx for the helpful comments on the paper.

■ ABREVIATIONS

K_S, switching equilibrium constant; K_D, dissociation constant; K_D^{App}, apparent dissociation constant; DR, dynamic range; n_H, Hill coefficient; k_{on}, association rate constant; k_{off}, dissociation rate constant; nt, nucleotide

■ REFERENCES

(1) Nel, A. E.; Mädler, L.; Velegol, D.; Xia, T.; Hoek, E. M. V.; Somasundaran, P.; Klaessig, F.; Castranova, V.; Thompson, M. Understanding biophysicochemical interactions at the nano−bio interface. *Nat. Mater.* **2009**, *8* (7), 543−557.

(2) Motlagh, H. N.; Wrabl, J. O.; Li, J.; Hilser, V. J. The ensemble nature of allostery. *Nature* **2014**, *508* (7496), 331−339.

(3) Ricci, F.; Vallée-Bélisle, A.; Porchetta, A.; Plaxco, K. W. Rational Design of Allosteric Inhibitors and Activators Using the Population-Shift Model: In Vitro Validation and Application to an Artificial Biosensor. *J. Am. Chem. Soc.* **2012**, *134* (37), 15177−15180.

(4) Simon, A. J.; Vallée-Bélisle, A.; Ricci, F.; Watkins, H. M.; Plaxco, K. W. Using the Population-Shift Mechanism to Rationally Introduce "Hill-type" Cooperativity into a Normally Non-Cooperative Receptor. *Angew. Chem., Int. Ed.* **2014**, *53* (36), 9471−9475.

(5) Simon, A. J.; Vallée-Bélisle, A.; Ricci, F.; Plaxco, K. W. Intrinsic disorder as a generalizable strategy for the rational design of highly responsive, allosterically cooperative receptors. *Proc. Natl. Acad. Sci. U.S.A.* **2014**, *111* (42), 15048−15053.

(6) Bissonnette, S.; Del Grosso, E.; Simon, A. J.; Plaxco, K. W.; Ricci, F.; Vallée-Bélisle, A. Optimizing the Specificity Window of Biomolecular Receptors Using Structure-Switching and Allostery. *ACS Sens.* **2020**, *5* (7), 1937−1942.

(7) Munzar, J. D.; Ng, A.; Juncker, D. Duplexed aptamers: history, design, theory, and application to biosensing. *Chem. Soc. Rev.* **2019**, *48* (5), 1390−1419.

(8) Porchetta, A.; Vallée-Bélisle, A.; Plaxco, K. W.; Ricci, F. Allosterically Tunable, DNA-Based Switches Triggered by Heavy Metals. *J. Am. Chem. Soc.* **2013**, *135* (36), 13238−13241.

(9) Porchetta, A.; Vallée-Bélisle, A.; Plaxco, K. W.; Ricci, F. Using Distal-Site Mutations and Allosteric Inhibition To Tune, Extend, and Narrow the Useful Dynamic Range of Aptamer-Based Sensors. *J. Am. Chem. Soc.* **2012**, *134* (51), 20601−20604.

(10) Rossetti, M.; Porchetta, A. Allosterically regulated DNA-based switches: From design to bioanalytical applications. *Anal. Chim. Acta* **2018**, *1012*, 30−41.

(11) Wodak, S. J.; Paci, E.; Dokholyan, N. V.; Berezovsky, I. N.; Horovitz, A.; Li, J.; Hilser, V. J.; Bahar, I.; Karanicolas, J.; Stock, G.; et al. Allostery in Its Many Disguises: From Theory to Applications. *Structure* **2019**, *27* (4), 566−578.

(12) Mariottini, D.; Idili, A.; Vallée-Bélisle, A.; Plaxco, K. W.; Ricci, F. A DNA Nanodevice That Loads and Releases a Cargo with Hemoglobin-Like Allosteric Control and Cooperativity. *Nano Lett.* **2017**, *17* (5), 3225−3230.

(13) Rossetti, M.; Ranallo, S.; Idili, A.; Palleschi, G.; Porchetta, A.; Ricci, F. Allosteric DNA nanoswitches for controlled release of a molecular cargo triggered by biological inputs. *Chem. Sci.* **2017**, *8* (2), 914−920.

(14) Del Grosso, E.; Ragazzon, G.; Prins, L. J.; Ricci, F. Fuel-Responsive Allosteric DNA-Based Aptamers for the Transient Release of ATP and Cocaine. *Angew. Chem., Int. Ed.* **2019**, *58* (17), 5582−5586.

(15) Porchetta, A.; Idili, A.; Vallée-Bélisle, A.; Ricci, F. General Strategy to Introduce pH-Induced Allostery in DNA-Based Receptors to Achieve Controlled Release of Ligands. *Nano Lett.* **2015**, *15* (7), 4467−4471.

(16) Whitty, A. Cooperativity and biological complexity. *Nat. Chem. Biol.* **2008**, *4* (8), 435−439.

(17) Williamson, J. R. Cooperativity in macromolecular assembly. *Nat. Chem. Biol.* **2008**, *4*, 458−465.

(18) Bai, Y.; Luo, Q.; Liu, J. Protein self-assembly via supramolecular strategies. *Chem. Soc. Rev.* **2016**, *45* (10), 2756−2767.

(19) Kitov, P. I.; Bundle, D. R. On the Nature of the Multivalency Effect: A Thermodynamic Model. *J. Am. Chem. Soc.* **2003**, *125* (52), 16271−16284.

(20) Hanebuth, M. A.; Kityk, R.; Fries, S. J.; Jain, A.; Kriel, A.; Albanese, V.; Frickey, T.; Peter, C.; Mayer, M. P.; Frydman, J.; et al. Multivalent contacts of the Hsp70 Ssb contribute to its architecture on ribosomes and nascent chain interaction. *Nat. Commun.* **2016**, *7* (1), 13695.

(21) Errington, W. J.; Bruncsics, B.; Sarkar, C. A. Mechanisms of noncanonical binding dynamics in multivalent protein−protein interactions. *Proc. Natl. Acad. Sci. U.S.A.* **2019**, *116* (51), 25659−25667.

(22) Cuesta, Á. M.; Sainz-Pastor, N.; Bonet, J.; Oliva, B.; Álvarez-Vallina, L. Multivalent antibodies: when design surpasses evolution. *Trends Biotechnol.* **2010**, *28* (7), 355−362.

(23) Vallée-Bélisle, A.; Ricci, F.; Plaxco, K. W. Thermodynamic basis for the optimization of binding-induced biomolecular switches and structure-switching biosensors. *Proc. Natl. Acad. Sci. U.S.A.* **2009**, *106* (33), 13802−13807.

(24) Hughes, R. A.; Ellington, A. D. Synthetic DNA Synthesis and Assembly: Putting the Synthetic in Synthetic Biology. *Cold Spring Harbor Perspect. Biol.* **2017**, *9* (1), a023812.

(25) Madsen, M.; Gothelf, K. V. Chemistries for DNA Nanotechnology. *Chem. Rev.* **2019**, *119* (10), 6384−6458.

(26) Seeman, N. C.; Sleiman, H. F. DNA nanotechnology. *Nat. Rev. Mater.* **2017**, *3* (1), 17068.

(27) Ricci, F.; Vallée-Bélisle, A.; Plaxco, K. W. High-Precision, In Vitro Validation of the Sequestration Mechanism for Generating Ultrasensitive Dose-Response Curves in Regulatory Networks. *PLoS Comput. Biol.* **2011**, *7* (10), No. e1002171.

(28) Ha, S. H.; Ferrell, J. E. Thresholds and ultrasensitivity from negative cooperativity. *Science* **2016**, *352* (6288), 990−993.

(29) Tyagi, S.; Kramer, F. R. Molecular Beacons: Probes that Fluoresce upon Hybridization. *Nat. Biotechnol.* **1996**, *14* (3), 303−308.

(30) Lauzon, D.; Vallée-Bélisle, A. Functional advantages of building nanosystems using multiple molecular components. *Nat. Chem.* **2023**, *15* (4), 458−467.

(31) Idili, A.; Ricci, F.; Vallée-Bélisle, A. Determining the folding and binding free energy of DNA-based nanodevices and nanoswitches using urea titration curves. *Nucleic Acids Res.* **2017**, *45* (13), 7571−7580.
(32) Esteban Fernández de Ávila, B.; Watkins, H. M.; Pingarrón, J. M.; Plaxco, K. W.; Palleschi, G.; Ricci, F. Determinants of the Detection Limit and Specificity of Surface-Based Biosensors. *Anal. Chem.* **2013**, *85* (14), 6593−6597.
(33) Hulme, E. C.; Trevethick, M. A. Ligand binding assays at equilibrium: validation and interpretation. *Br. J. Pharmacol.* **2010**, *161* (6), 1219−1237.
(34) Chen, X. Expanding the Rule Set of DNA Circuitry with Associative Toehold Activation. *J. Am. Chem. Soc.* **2012**, *134* (1), 263−271.
(35) Ang, Y. S.; Yung, L.-Y. L. Dynamically elongated associative toehold for tuning DNA circuit kinetics and thermodynamics. *Nucleic Acids Res.* **2021**, *49* (8), 4258−4265.
(36) Vallée-Bélisle, A.; Ricci, F.; Plaxco, K. W. Engineering Biosensors with Extended, Narrowed, or Arbitrarily Edited Dynamic Range. *J. Am. Chem. Soc.* **2012**, *134* (6), 2876−2879.
(37) Ricci, F.; Vallée-Bélisle, A.; Simon, A. J.; Porchetta, A.; Plaxco, K. W. Using Nature's "Tricks" To Rationally Tune the Binding Properties of Biomolecular Receptors. *Acc. Chem. Res.* **2016**, *49* (9), 1884−1892.
(38) Ortega, G.; Chamorro-Garcia, A.; Ricci, F.; Plaxco, K. W. On the Rational Design of Cooperative Receptors. *Annu. Rev. Biophys.* **2023**, *52* (1), 319−337.
(39) Vallée-Bélisle, A.; Ricci, F.; Uzawa, T.; Xia, F.; Plaxco, K. W. Bioelectrochemical Switches for the Quantitative Detection of Antibodies Directly in Whole Blood. *J. Am. Chem. Soc.* **2012**, *134* (37), 15197−15200.
(40) Bracaglia, S.; Ranallo, S.; Plaxco, K. W.; Ricci, F. Programmable, Multiplexed DNA Circuits Supporting Clinically Relevant, Electrochemical Antibody Detection. *ACS Sens.* **2021**, *6* (6), 2442−2448.
(41) Ranallo, S.; Sorrentino, D.; Ricci, F. Orthogonal regulation of DNA nanostructure self-assembly and disassembly using antibodies. *Nat. Commun.* **2019**, *10* (1), 5509.
(42) Engelen, W.; Meijer, L. H. H.; Somers, B.; de Greef, T. F. A.; Merkx, M. Antibody-controlled actuation of DNA-based molecular circuits. *Nat. Commun.* **2017**, *8* (1), 14473.
(43) Liang, H.; Chen, S.; Li, P.; Wang, L.; Li, J.; Li, J.; Yang, H.-H.; Tan, W. Nongenetic Approach for Imaging Protein Dimerization by Aptamer Recognition and Proximity-Induced DNA Assembly. *J. Am. Chem. Soc.* **2018**, *140* (12), 4186−4190.
(44) Mocenigo, M.; Porchetta, A.; Rossetti, M.; Brass, E.; Tonini, L.; Puzzi, L.; Tagliabue, E.; Triulzi, T.; Marini, B.; Ricci, F.; et al. Rapid, Cost-Effective Peptide/Nucleic Acid-Based Platform for Therapeutic Antibody Monitoring in Clinical Samples. *ACS Sens.* **2020**, *5* (10), 3109−3115.
(45) Hasegawa, H.; Taira, K.-i.; Sode, K.; Ikebukuro, K. Improvement of Aptamer Affinity by Dimerization. *Sensors* **2008**, *8* (2), 1090−1098.
(46) Hu, X.; Tang, L.; Zheng, M.; Liu, J.; Zhang, Z.; Li, Z.; Yang, Q.; Xiang, S.; Fang, L.; Ren, Q.; et al. Structure-Guided Designing Pre-Organization in Bivalent Aptamers. *J. Am. Chem. Soc.* **2022**, *144* (10), 4507−4514.
(47) Riccardi, C.; Napolitano, E.; Musumeci, D.; Montesarchio, D. Dimeric and Multimeric DNA Aptamers for Highly Effective Protein Recognition. *Molecules* **2020**, *25* (22), 5227.
(48) Debiais, M.; Lelievre, A.; Smietana, M.; Müller, S. Splitting aptamers and nucleic acid enzymes for the development of advanced biosensors. *Nucleic Acids Res.* **2020**, *48* (7), 3400−3422.
(49) Bertucci, A.; Porchetta, A.; Ricci, F. Antibody-Templated Assembly of an RNA Mimic of Green Fluorescent Protein. *Anal. Chem.* **2018**, *90* (2), 1049−1053.
(50) Harroun, S. G.; Prévost-Tremblay, C.; Lauzon, D.; Desrosiers, A.; Wang, X.; Pedro, L.; Vallée-Bélisle, A. Programmable DNA switches and their applications. *Nanoscale* **2018**, *10* (10), 4607−4641.
(51) Lauzon, D.; Zhu, G.; Vallée-Bélisle, A. Engineering DNA Switches for DNA Computing Applications. *DNA- and RNA-Based Computing Systems*, 2021, pp 105−124.
(52) Shekhawat, S. S.; Ghosh, I. Split-protein systems: beyond binary protein−protein interactions. *Curr. Opin. Chem. Biol.* **2011**, *15* (6), 789−797.
(53) Ranallo, S.; Prévost-Tremblay, C.; Idili, A.; Vallée-Bélisle, A.; Ricci, F. Antibody-powered nucleic acid release using a DNA-based nanomachine. *Nat. Commun.* **2017**, *8* (1), 15150.
(54) Békés, M.; Langley, D. R.; Crews, C. M. PROTAC targeted protein degraders: the past is prologue. *Nat. Rev. Drug Discovery* **2022**, *21* (3), 181−200.
(55) Copeland, R. A. The drug−target residence time model: a 10-year retrospective. *Nat. Rev. Drug Discovery* **2016**, *15* (2), 87−95.
(56) Del Bianco, C.; Aster, J. C.; Blacklow, S. C. Mutational and Energetic Studies of Notch1 Transcription Complexes. *J. Mol. Biol.* **2008**, *376* (1), 131−140.
(57) Recht, M. I.; Williamson, J. R. RNA Tertiary Structure and Cooperative Assembly of a Large Ribonucleoprotein Complex. *J. Mol. Biol.* **2004**, *344* (2), 395−407.
(58) Courey, A. J. Cooperativity in transcriptional control. *Curr. Biol.* **2001**, *11* (7), R250−R252.

https://doi.org/10.1021/jacs.3c04045
J. Am. Chem. Soc. XXXX, XXX, XXX−XXX